Advances in Nano Research, *Vol. 10, No. 4 (2021) 373-383*
DOI: https://doi.org/10.12989/anr.2021.10.4.373

Silver (I)- Schiff-base complex intercalated layered double hydroxide with antimicrobial activity

Mary Jenisha Barnabas [a], Surendran Parambadath [b], Saravanan Nagappan [c], Ildoo Chung [d] and Chang-Sik Ha*

Department of Polymer Science and Engineering, School of Chemical Engineering, Pusan National University, Geumjeong-gu, Busan, 46241, Republic of Korea

(*Received December 26, 2018, Revised November 20, 2020, Accepted January 2, 2021*)

Abstract. In this work, silver nitrate complexes of sulfanilamide-5-methyl-2-thiophene carboxaldehyde (SMTCA) ligand intercalated Zn/Al-layered double hydroxide [Ag-SMTCA-LDH] were synthesized for the potential application as an antimicrobial system. The SMTCA ligand was synthesized by reacting sulfanilamide and 5-methyl-2-thiophene carboxaldehyde in methanol and further complexation with silver nitrate metal ions [Ag-SMTCA]. The structural analyses of synthesized compounds confirmed an intercalation of Ag-SMTCA into Zn/Al-NO_3-LDH by flake/restacking method. SMTCA, Ag-SMTCA and Ag-SMTCA-LDH were characterized by ^{1}H nuclear magnetic resonance (^{1}H NMR) spectroscopy, Fourier-transform infrared (FTIR), ultraviolet-visible (UV-Vis) spectrophotometer, scanning electron microscopy (SEM) and transmission electron microscopy (TEM), X-ray diffraction (XRD), and thermogravimetric analysis (TGA). It was found that Ag-SMTCA-LDH exhibited good antimicrobial activity against both gram-positive (*Bacillus subtilis*, [*B. subtilis*], *Staphylococcus aures*, [*S. aureus*]) and gram-negative (*Escherichia coli*, [*E. coli*], *Pseudomonas aeruginosa* [*P. aeroginosa*]) bacteria as well as excellent antioxidant activity.

Keywords: Schiff-base complex; layered double hydroxide; silver; antimicrobial activity; antioxidant activity

1. Introduction

5-methyl-2-thiophene carboxaldehyde is a natural and hydrophilic antimicrobial compound for various applications such as pharmaceutical, food, and wood preservation (Harinath *et al*. 2013). Its vigorous odor and immense volatility, however, limit its diverse applications. Furthermore, sulfa drugs are referred to as the type of drugs that act as therapeutic and protective against several bacterial infections such as eye infection, influenza, meningitis, actinomics infections, urinary tract diseases, and have been used as model compounds to reveal the mechanisms for the action of drugs. In particular, sulfanilamide, the first drug among such sulfa drugs, has been found to operative consistently and selectively as preventive and therapeutic assistant against distinct diseases (Ganesh *et al*. 2016, Keshk *et al*. 2016, Barnabas *et al*. 2017).

Schiff base and its derivatives are utilized as insecticides and fungicides, as good flavoring agent for liquor and bouquet, as decomposition inhibition factor for ferrous mixture in corrosive fluids (Caboni *et al*. 2012, Ingale *et al*. 2015, Cohen *et al*. 2017). Schiff base ligands are treated as powerful ligands, because they are easily synthesized via a simple one-pot condensation of aldehydes and alcohol solvent containing primary amine (Buey *et al*. 1998). The biologically active metal complex is synthesized by using nitrogen and sulphur present in the ring system of heterocyclic compounds. Metal complexes of Schiff bases have various applications along with their antifungal, antiviral, and antibacterial actions. Metal complexes of Schiff base ligands are ubiquitous because of their effective synthesis, wide applications, and the accessibility of divergent structural modifications (Delahaye *et al*. 2010, Kursunlu *et al*. 2019).

On the other hand, layered double hydroxides (LDHs) are bidimensional solids with plenty of positive charge with their brucite like layers (Isa *et al*. 2013). LDHs have the structural formula, $[M^{2+}_{1-x}M^{3+}_{x}(OH)_2](A^{m-})_{x/m}\cdot nH_2O$, where M^{2+} or M^{3+} are divalent or trivalent metal cations, respectively, A^{m-} is an interlayer *m*-valent anion, and x ranges from 0.17 to 0.33. LDHs showed excellent metal adsorption behaviour from aqueous solution due to the presence of positive charges in the surface layer and high surface area (Barbosa *et al*. 2002). The mechanism behind LDHs is due to the positive charge reaction, which enables the hydroxide ions encompassed by the exterior of the LDH minerals in solution to form metal hydroxides.

Intercalation is a well-known methodology used for the insertion of various organic compounds into the interlayer of anionic clay or hydrotalcite-like compounds, for potential

*Corresponding author, Ph.D., Professor,
E-mail: csha@pnu.edu
[a] Ph.D., E-mail: bmaryjenisha@gmail.com
[b] Ph.D., E-mail: srpcat@gmail.com
[c] Ph.D., E-mail: saravananagappan@gmail.com
[d] Professor, E-mail: idchung@pusan.ac.kr

ISSN: 2287-237X (Print), 2287-2388 (Online)

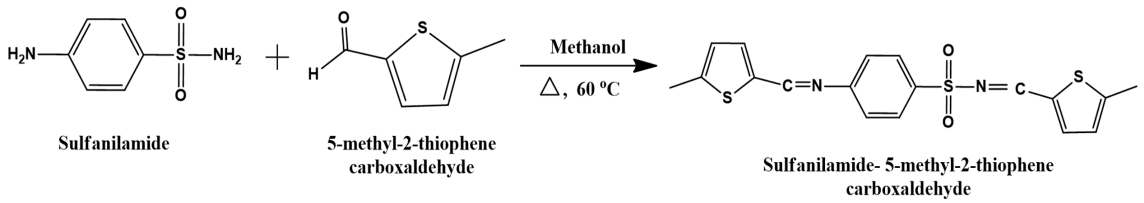

Scheme 1. Preparation of 5-methyl-2-thiphene carboxaldehyde-Sulfanilamide Schiff base ligand (SMTCA).

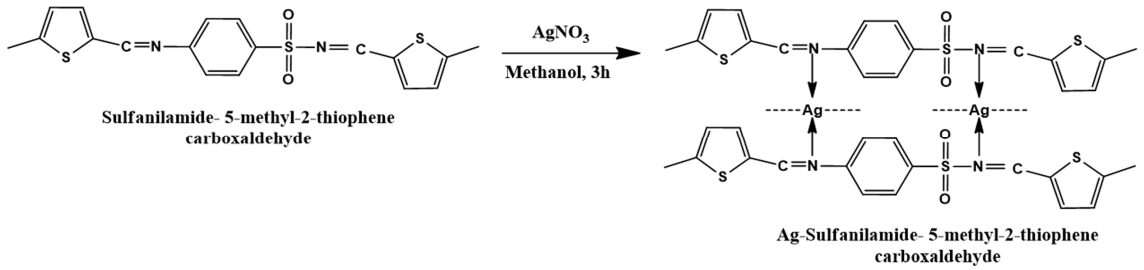

Scheme 2. Preparation of silver complexes of SMTCA ligand (Ag-SMTCA).

applications. In particular, recent studies focused on the poorly water-soluble drug intercalated LDHs attracted much interest (Marcato *et al*. 2013, Barnabas *et al*. 2017). In this sense, Schiff base complex-intercalated LDH was extensively investigated (Ukrainczyk *et al*. 1994, Zhang *et al*. 2005, Shi *et al*. 2010, Wang *et al*. 2013, Parida *et al*. 2016).

In addition, silver nanoparticles have high potential antibacterial activity against a variety of bacteria even at a very low concentration (Goss *et al*. 2003, Ray *et al*. 2007, Prabhu and Poulose 2012, Vanaja and Gurusamy 2012, Savic *et al*. 2016, Ganesh *et al*. 2016, Ding *et al*. 2017). Silver nanoparticles employed in a LDH matrix have an advantage in that the release of silver nanoparticles for longer periods is enhanced, avoiding toxicity to normal cells.

Taking all the aforementioned aspects into consideration, in this study, therefore, we aimed to synthesize functional Schiff base ligands using sulfanilamide and 5-methyl-2-thiophene carboxaldehyde and form their complexes with Ag(I), which were intercalated into Zn/Al-LDHs. We also investigated antimicrobial activities of the LDHs with Ag(I) complexed Schiff base ligands against either gram-positive or gram-negative bacteria's as well as their antioxidant activities.

2. Experimental

2.1 Materials and Methods

Silver nitrate, aluminium(III) nitrate nonahydrate, zinc(II) nitrate hexahydrate, sulfanilamide, 5-methyl-2-thiophene carboxaldehyde, and sodium hydroxide (NaOH) were purchased from Sigma-Aldrich and used as received.

2.2 Synthesis of [Sulfanilamide-5-methyl-2-thiophene carboxaldehyde] (SMTCA)

5-Methyl-2-thiophene carboxaldehyde (2 mmol, 0.254 g) was taken in a 250 ml round flask and dissolved in 50 ml absolute methanol under stirring at 80 rpm. Similarly, sulfanilamide (2 mmol, 0.254 g) was dissolved in 50 ml absolute methanol, which was added to the above solution by drop-wise addition with stirring under reflux for 6 h at 60°C. The color of the solution was changed to yellow during stirring and the obtained solid precipitate was isolated. The material was filtered and washed with cold methanol several times and dried for overnight (see Scheme 1).

2.3 Synthesis of Ag-SMTCA complex

The hydrate metal complex was prepared by reacting 0.295 g (1.0 mmol) of $AgNO_3$ and 0.354 g (1 mmol) of the synthesized Schiff base ligand at a metal to ligand molar ratio of 1:2. The metal solution was added drop by drop to a hot solution of ligand (60°C) in methanol and refluxed further for 3 h. The reaction mixture was filtered, washed with methanol and dried at 50°C by using vacuum for 1 h. (see Scheme 2).

2.4 Synthesis of Zn-Al-LDH

Co-precipitation method was employed for the synthesis of Zn-Al-LDH according to the previous literature (Isa *et al*. 2013). Initially, a mixture of metal nitrate solution was prepared by mixing 0.5 M Zn^{2+} and 0.3 M Al^{3+} and then the pH of the solution was adjusted to pH 9-10 with addition of the required amount of 2 M NaOH. The obtained mixture was kept at 60°C for 24 h under stirring and cooled to room temperature. The white precipitate formed by this procedure was filtered, followed by washing with de-ionised water, and dried at 80°C for overnight. The pick-up material was ground smoothly into a fine powder.

2.5 Intercalation of metal complex into Zn-Al-LDH

Zn/Al-LDH (0.075 g) was added to 30 mml formamide and stored for 24 h, which was then changed to a translucent

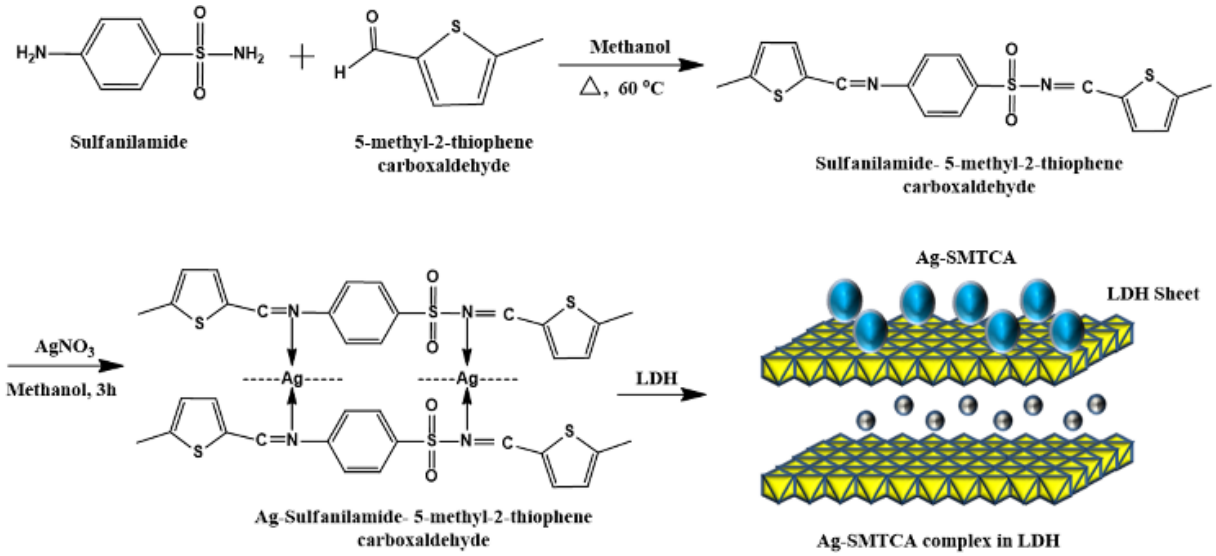

Scheme 3. Intercalation of Ag-SMTCA into layered double hydroxide (Ag-SMTCA-LDH).

colloidal suspension in 24 h. Ag-SMTCA complex (0.4 g) in 25 ml methanol was added to the colloidal suspension, where the translucent suspension was immediately changed to cloudy one. Then the cloudy suspension was stirred hardily for 24 h, stored at 60°C for 48 h, and then cooled to room temperature. The resulted intercalated materials were designated as Ag-SMTCA-LDH (see Scheme 3).

2.6 Antimicrobial study

The in-vitro antimicrobial screening test of the Ag-SMTCA-LDH was done both for gram-positive *B. subtilis*, *S. aureus* and gram-negative *E. coli*, *P. aeroginosa* microorganisms. The compounds were stored to dry at room temperature and dissolved in dimethyl formamide (DMF). The sterilized nutrient agar (NA) medium was solidified on petri dishes. 100 µl of bacterial cultures (*B. subtilis*, *S. aureus* and *E. coli*, *P. aeroginosa*) were streaked on the surface of the solidified NA medium. Different concentrations (25, 50 and 100 µg/mL) of Ag-SMTCA-LDH solutions were prepared in DMF and loaded into a sterilized paper disk with 6 mm diameter. The bacterial cultures with samples were incubated for 24 h at 37ºC in the incubation chamber (Khanye *et al*. 2011). Then inhibition zones (DIZ) appeared around the samples disk were measured in millimetre as antibacterial effect of Ag-SMTCA-LDH. Three times of measurement was averaged.

2.7 DPPH (2,2-diphenyl-1-picryl-hydrazyl-hydrate) radical scavenging analysis

The scavenging effect on DPPH radical was investigated by using different sample concentration according to the previous method (Pan *et al*. 2008); extract solution, 0.2 mL; 95% ethanol at various concentrations; 0.004% (w/v) of 8 mL stock solution of DPPH in ethanol (95%); Ag-SMTCA-LDH of five different concentrations (100, 200, 300, 400, 500 mg mL^{-1}); Evaluating UV-vis absorbance at 517 nm; Ascorbic acid for the act of positive control. The DPPH free radical scavenging action was determined by the following equation.

$$\text{DPPH scavenging effect (\%)} = [(A_0 - A_t)/A_0] \times 100$$

where A_0 is the absorbance of the control and A_t is the absorbance of the sample. More details of the DPPH radical scavenging analysis are described in the literature (Khoo *et al*. 2014).

2.8 Characterization

Powder X-ray diffraction (XRD, Bruker AXN) was conducted using Ni-filtered CuKα radiation (λ = 0.15418 nm) at 40 kV and 40 mA in order to reveal the crystalline structure of the synthesized materials (Kong *et al*. 2010). The XRD patterns were collected in the wide-angle range from 10° to 60° 2θ. The ^{1}H NMR (Bruker DSX 400) spectra were obtained to reveal the nature of ligand using a 4 mm zirconia rotor spinning at 6 kHz. ^{1}H NMR spectra were recorded in deuterated dimethyl sulfoxide (DMSO-d_6) with a small amount of tetramethylsilane (TMS) as an internal standard. Fourier transform infrared (FTIR, JASCO FTIR 4100) spectroscopy was used to identify the functional groups present in the materials using KBr pellets over the frequency range, 4000 – 400 cm^{-1} with 2 cm^{-1} resolution. Scanning electron microscopy (SEM, JEOL 6400) images were obtained after thin gold film coating to check the surface morphology at an acceleration voltage of 20 kV. Transmission electron microscopy (TEM, JEOL 2010) images were obtained at an accelerating voltage of 200 kV to check the morphology of samples in depth. Thermogravimetric analysis (TGA, Perkin Elmer Pyris Diamond) was done to check the thermal stability with the controlled heating rate (10°C min^{-1}) under nitrogen atmosphere. The ultraviolet (UV) absorption spectra of the samples were recorded for measuring the absorbance values to reveal the complex nature of ligand in depth as well as the antioxidant activity using a UV-visible spectrophotometer (U- 2010, HITACHI Co.).

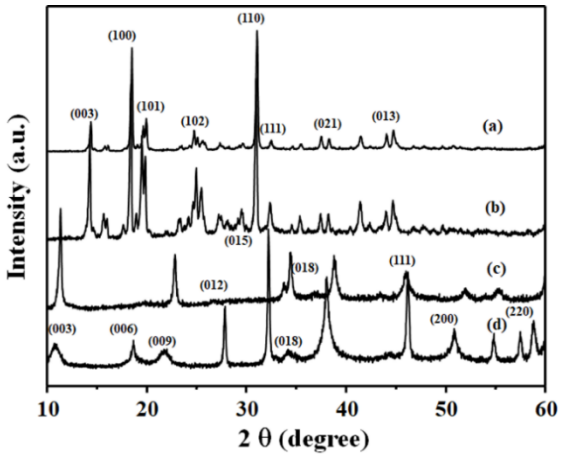

Fig. 1 XRD patterns of (a) SMTCA; (b) Ag-SMTCA; (c) pure-Zn/Al-LDH; and (d) Ag-SMTCA-LDH complex.

3. Results and discussion

3.1 Characterization of SMTCA, Ag-SMTCA, Zn/Al-LDH, and Ag-SMTCA-LDH

3.1.1 XRD analysis

Figs. 1(a) and (b) show the powder X-ray diffraction (XRD) patterns of SMTCA (Fig. 1(a)) and the metal complex (Ag-SMTCA, Fig. 1(b)). The free ligand clearly showed three sharp peaks at the 2θ positions of 14.4°, 18.50°, and 31.1°. The SMTCA ligand showed several weak crystalline peaks at 2θ position of 15.8°, 20.0°, 23.5°, 24.7°, 25.7°, 27.4°, 29.6°, 32.5°, 34.7°, 35.4°, 37.5°, 38.3°, 41.5°, 44.1°, and 44.8°. The obtained peaks illustrate the crystalline nature of the synthesized SMTCA ligand. The XRD pattern of the metal complex (Ag-SMTCA) showed almost similar peaks as that of SMTCA ligand as well as the four distinct diffraction peaks at 38.1°, 44.1°, and 47.8° that can be assigned as (111), (200), and (220) planes, respectively, of the fcc crystalline structure of Ag (Ji *et al*. 2015). It is seen that the peak intensities of Ag-SMTCA complex was increased as compared to that of SMTCA, meaning enhanced crystalline behavior of the metal complex (Fig. 1(b)) (Kursunlu *et al*. 2009).

In general, high crystallinity with a typical hydrotalcite structure is observed for the Zn/Al-LDHs prepared by co-precipitation method, whereas a little lower degree of crystallinity is observed for the Zn-Al-LDHs when they are prepared by the reconstruction method (Marcato *et al*. 2013). The XRD pattern of Zn/Al-LDH (Fig. 1(c)) shows several sharp and intense peaks in the 2θ angles at 11.3°, 22.9°, 34.5°, 38.8°, 46.1°, 52.0°, and 55.5°, which are attributed to (003), (006), (009), (015), (018), (110) and (113) planes of the typical well-crystalized hydrotalcite-like LDH materials (Zhang *et al*. 2005, 2016, Zhao *et al*. 2012, Abderrazek *et al*. 2016, Yuan *et al*. 2017). The typical X-ray patterns of LDHs containing basal (003) reflections are related to the hydroxide layers of Zn/Al-LDHs (Cohen *et al*. 2017, Mishra *et al*. 2013). The XRD pattern of Ag/SMTCA-LDH nanocomposites showed sharp and weak crystalline peaks in the 2θ angles at 10.8°, 18.6°, 21.8°, 27.9°, 32.3°, 34.1°, 38.0°, 46.2°, 50.9°, 54.9°, 57.5°, and 58.7° (Fig. 1(d)), which exhibits the combined crystalline structure of both Ag-SMTCA and Zn/Al-LDH. It is interesting to note that the crystalline structure of Ag such as (111), (200), and (220) planes is noticeably observed for Ag-SMTCA-LDH (Ji *et al*. 2015), while it is not clearly observed for Ag-SMTCA if one compares Figs. 1(b) and (d). The result is due to the fact that 1:2 molar ratio of metal to ligand was used to prepare Ag-SMTCA, while large excess of Ag-SMTCA to Zn/Al-LDH (ca. 5 times based on weight %) was used to intercalate Zn/Al-LDH into the Ag-SMTCA. The 2θ values of (003) and (018) diffractions of Ag-SMTCA-LDH nanocomposites exhibited a small shift to lower angles when compared to those of Ag-SMTCA and Zn/Al-LDH, respectively, with the appearance of new peaks in addition to the disappearance of some peaks due to both Ag-SMTCA and Zn/Al-LDH, which were due to somewhat the intercalation of the Ag-SMTCA ligand into Zn/Al-LDH, acknowledging good agreement with those from literatures (Nocchetti *et al*. 2013, Noh *et al*. 2012).

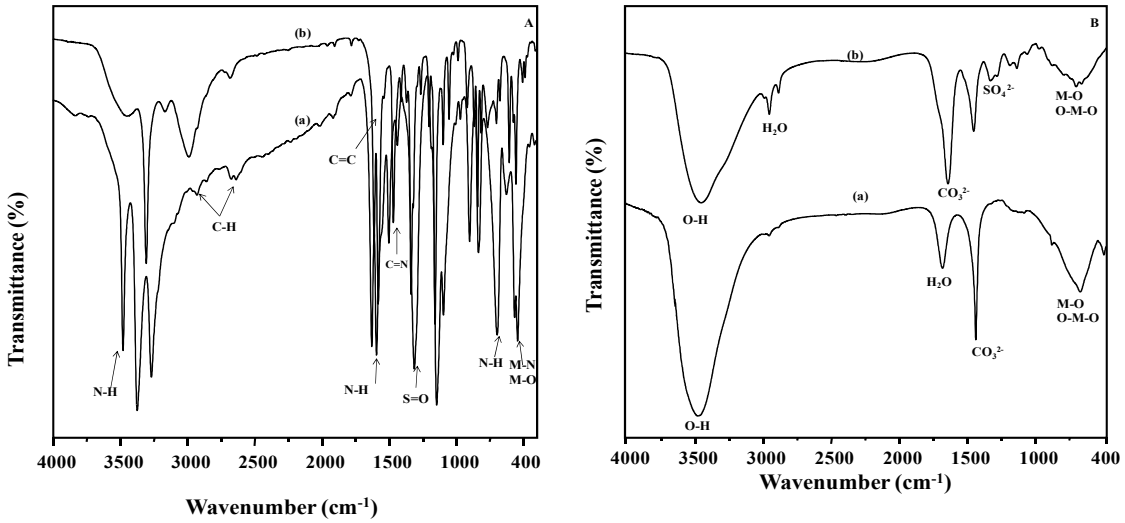

Fig. 2 FT-IR spectra of [A] (a) SMTCA; and (b) Ag-SMTCA; and [B] (a) Zn/Al-LDH; and (b) Ag-SMTCH-LDH complex.

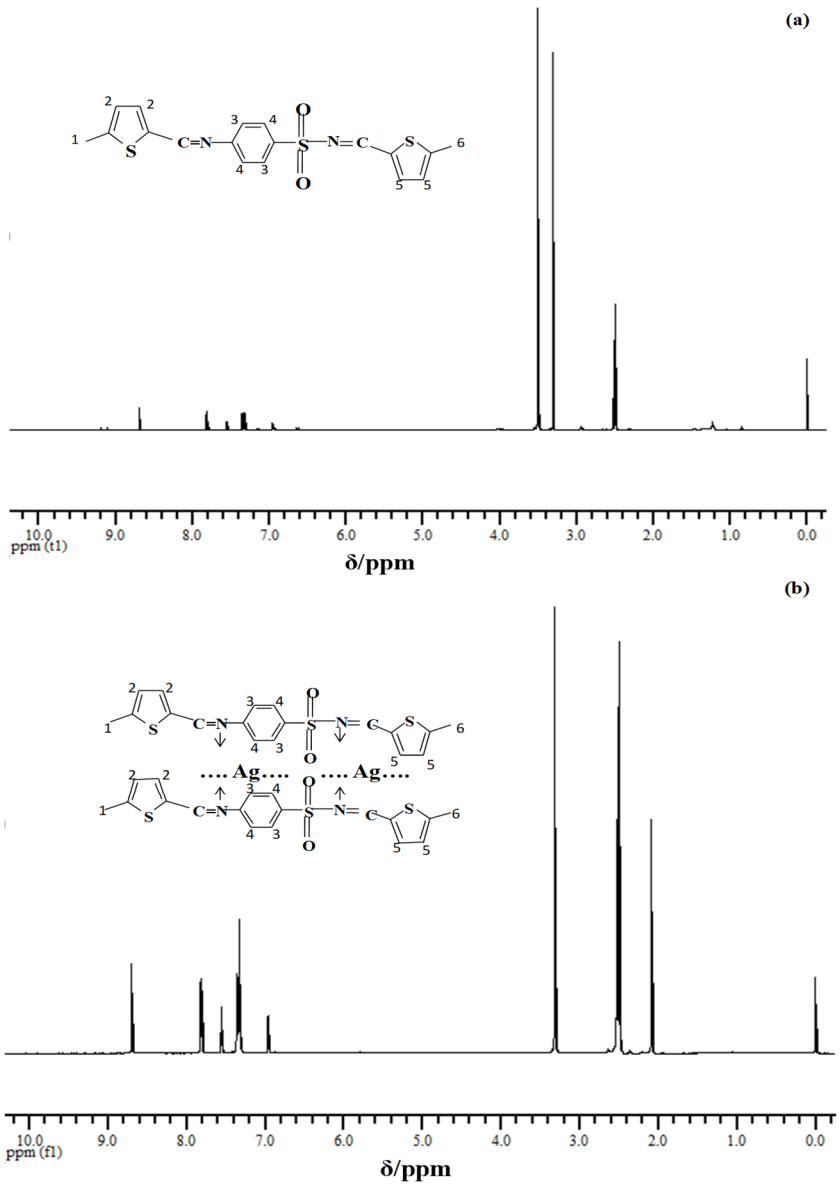

Fig. 3 ^{1}H NMR spectra of (a) SMTCA; and (b) Ag-SMTCA complex.

3.1.2 FTIR analysis

Fig. 2A(a) shows the FTIR spectra of (a) SMTCA and (b) Ag-SMTCA samples. The pure ligand exhibited the characteristic vibrational bands of -CH, C=C, C=N, and S=O groups (Fig. 2A(a)). The vibrational frequencies of the above functional moieties were persisted even after the complexation with silver nitrate ions (Fig. 2A(b)).

The FTIR spectrum (KBr) of SMTCA showed characteristic absorption peaks at 1690 cm^{-1} (imino group) and 1320 cm^{-1} / 1150 cm^{-1} (sulfonyl group). The -CH stretching vibrations of the methyl group present in the SMTCA were also identified in the wavenumbers between 3000 and 2850 cm^{-1} (Nunes *et al*. 2015). Furthermore, the FTIR spectrum of the metal complex showed new strong vibrating peaks around 445 cm^{-1}, proving the presence of metal-nitrogen (M-N) and metal-oxide (M-O) bonds in the Ag-SMTCA complex.

Fig. 2B(a) illustrates the FTIR spectrum of the Zn/Al-LDH sample. The ν_3 vibration signal of CO_3^{2-} is observed at 1384 cm^{-1}. The stretching vibrations of hydroxyl groups and water in the surface and interlayer were observed with the broad band center at 3451 cm^{-1}**.** The absorption peak of O-H stretching in free water is observed usually at 3600 cm^{-1}, while the shift to a lower frequency in LDHs suggests the formation of hydrogen bonds between water in the interlayer and guest anions and/or with the layer hydroxide groups. The weak band at 1638 cm^{-1} is due to a bending mode of water molecules. The presence of M-O and O-M-O groups can be also proved from the vibration bands at 446 and 672 cm^{-1}. The existence of the above spectral vibrations with decreased intensities in the spectrum in comparison to that before complexation revealed the presence of Ag-SMTCA complex in the interlayer cavity of Zn/Al-LDH (Fig. 2B(b)) This is the preliminary analytical evidence for the intercalation of the Ag-SMTCA complex into the Zn/Al-LDH gallery.

Table 1 ^{1}H NMR spectral data of ligand (SMTCA) with its (Ag-SMTCA) complexes (unit; ppm).

Ligand/Complex	Thiophene proton	Imine proton	Methyl proton	Aldehyde proton	Acetate
SMTCA	7.8	8.7	3.4	9.8	-
Ag-SMTCA	-	8.7	-	-	2.1

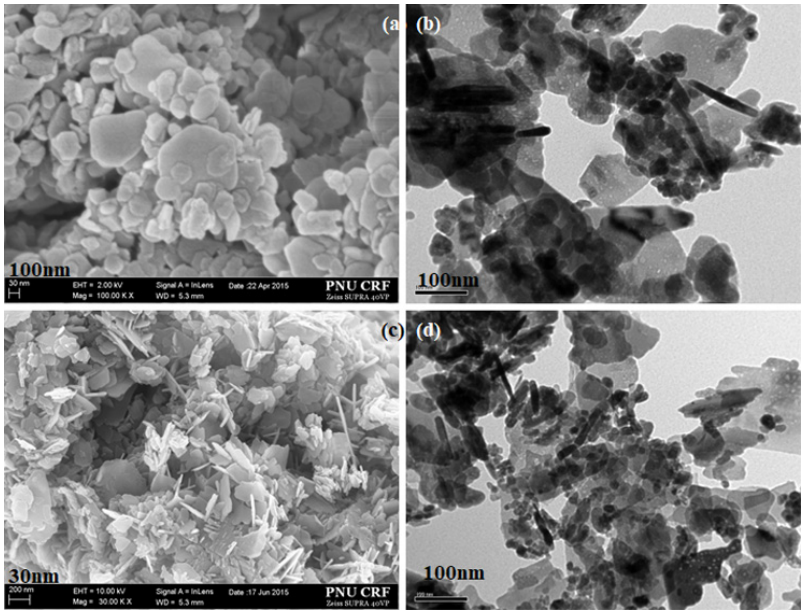

Fig. 4 SEM and TEM images of Zn/Al-LDH [(a) and (b)]; and Ag-SMTCA-LDH [(c) and (d)], respectively.

3.1.3 ^{1}H NMR spectra

In Fig. 3, the ^{1}H NMR spectrum of SMTCA shows signals of aromatic and thiophenicprotons at δ 7~8 ppm, imine protons at δ 8.7 ppm, and methyl protons at δ 3.4 ppm with the concurrent disappearance of signals of aldehyde protons at 9.8 ppm (Rani and Mohamad 2014). In Ag-SMTCA complexes, the signal from imine proton was also observed at δ 8.7 ppm, and the appearance of a new signal at δ 2.1 ppm are due to the presence of three proton integrals which are the characteristic of acetate metal coordination. In this way, the bidentate nature of ligand can be proved from the ^{1}H NMR spectra (Table 1).

3.1.4 SEM and TEM analysis

The SEM and TEM images for the Zn/Al-LDH are illustrated in Figs. 4(a) and (b), respectively. The micrographs show a relatively narrow particle size distribution (50-500 nm) and aggregates of dense and non-porous plate-like structures, which is in accordance with an LDH particle. Furthermore, the crystal morphology of intercalated compounds was not significantly affected, as observed in the XRD patterns.

Similar morphology was observed in the TEM images of the Zn/Al-LDH with the plate-like structure and the size ranging from 30-500 nm (Cohen *et al*. 2017, Ray *et al*. 2007). This kind of plate-like structure was already reported elsewhere (Zhang *et al*. 2016, Abderrazek *et al*. 2016, Yuan *et al*. 2017). Figs. 4(c) and (d) present the SEM and TEM images of Ag-SMTCA-LDH, respectively. A plate-like morphology was noticed for the pristine Zn/Al-LDH, while a sheet-like morphology was observed after preparing intercalated Ag-SMTCA-LDH, whose average particle size was ca. 100 nm.

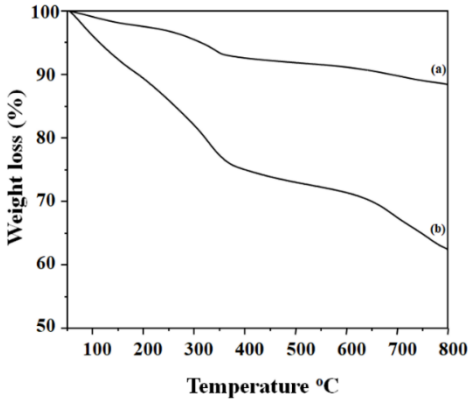

Fig. 5 TGA curves of (a) Zn/Al-LDH; and (b) Ag-SMTCA-LDH.

3.1.5 TGA curves

TGA curves of (a) Zn/Al-LDH and (b) Ag-SMTCA-LDH were presented in Fig. 5. For LDHs, the initial two step weight losses were observed due to physically adsorbed water at 30-100°C (2.37% mass loss) and the dihydroxylation of the brucite-like layers at 100-250°C (13.69% mass loss), respectively. The 24.99% mass loss around 250-500°C is attributed to the decomposition of nitrate anions. The complete decomposition of LDH can be observed with the last weight loss (500-800°C, 4.57% mass loss). The sharp degradation around 100°C is coming from

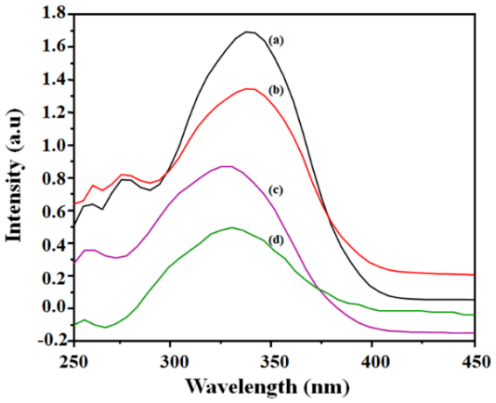

Fig. 6 UV-vis spectra of (a) SMTCA; (b) Ag-SMTCA; (c) Zn/Al-LDH; and (d) Ag-SMTCA-LDH.

the loss of physically absorbed water and the weight loss was found to be 7%.

A gradual weight loss in between 100 and 350°C, which was predicted to 5%, is due to the elimination of crystal water and the metamorphism. On the other hand, the materials exhibited distinct weight loss in between 350 and 800°C, indicating the decomposition of organic complex from the intercalated cavity, followed by steady weight loss. The total organic functionality in both materials were estimated at 24 wt.% for Ag-SMTCA-LDH.

3.1.6 UV-vis spectroscopic analysis

In Fig. 6, two distinct regions were observed for the ligand complex and intercalated LDH on UV-vis spectra in the range of 250-450 nm. In general, the electronic intra-ligand transitions are detected in the range of 250-400 nm and the d-d transition is encountered at higher wavelength. The spectrum of the complex mostly shows the important bands of the free ligand with minor modification of band wavelength and intensity as well as the appearance of new bands at higher wavelengths. The three bands in the region of 250-400 nm for SMTCA and the complex are attributed to the $\sigma \rightarrow \sigma^*$, $\pi \rightarrow \pi^*$ or $n \rightarrow \pi^*$ transitions, respectively. (Ran *et al*. 2011) Furthermore, the weak broad band in the region of 400-450 nm for Ag(I) complex is due to the $^4A_2$ (F) $\rightarrow$ $^4T_1$(F) transition, suggesting tetrahedral geometry for the silver nitrate complex. The UV-vis spectrum of the Ag-SMTCA-LDH complex that is similar to the free complex suggests that the complex has been shielded by LDH during intercalation, since LDH shows high reflectance in visible region (Shebl *et al*. 2010).

3.1.7 Antibacterial properties

Antibacterial properties of materials are quite important for end uses in industrial applications such as food packaging and drug delivery system, and so on (Sharaby 2007, Rani and Mohamad 2014, Rubino *et al*. 2017). In this sense, it is well known that both Zn and Zn/Al-LDH as well as Ag and Ag-LDH exhibit excellent antibacterial activities (Dibrov *et al*. 2002, Noh *et al*. 2012, Nocchetti *et al*. 2013, Mishra *et al*. 2013, Rasouli *et al*. 2017, Peng *et al*. 2018). The Schiff base complex was also known to show good antibacterial activity (Shebl *et al*. 2010, Ahmadi and Amani 2012, Jamuna *et al*. 2012, Wang and Zhang 2012, Khoo *et al*. 2014, Nunes *et al*. 2015, Ingale *et al*. 2015, Salehi *et al*. 2016, Zanvettor *et al*. 2016, Wang *et al*. 2016, Ozbek *et al*. 2017). In the present work, we focused only the antibacterial activity of the final resultant material, Ag-SMTCA-LDH composites, since good antibacterial activities of other materials such as Schiff base complex, Ag-Schiff base complex, and LDH are already well documented as mentioned above. The antimicrobial activity of the prepared Ag-SMTCA-LDH composites against *Bacillus substilis*, *Staphylococcus aureus* (gram-positive) and *Escherichia coli*, *Pseudomonas aeroginosa* (gram-

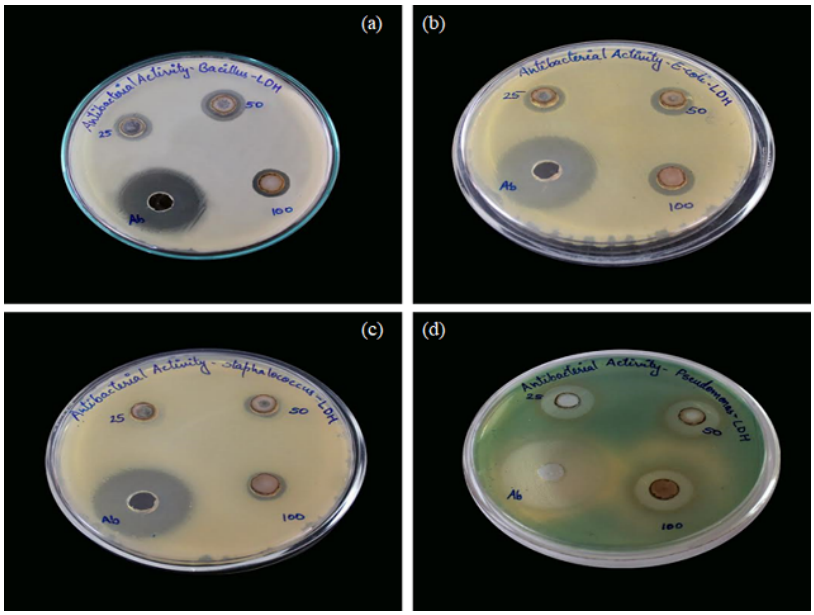

Fig. 7 Antibacterial activity of (a) *B. subtilis*; (b) *E. coli*; (c) *S. aureus*; and (d) *P. aeroginosa* at various concentrations (25, 50, 100 µg/mL) of Ag-SMTCA-LDH. The numerical values to compare the different antibacterial activity which are measured from these images are listed in Table 2.

Table 2 Antimicrobial activity of Ag-SMTCA-LDH.

Material	Concentration (μg/mL)	Antibacterial activity (in terms of DIZ in mm)			
		B. subtilis	*S. aureus*	*P. aeruginosa*	*E. coli*
Ag-SMTCA-LDH	25	10	0	16	12
	50	11	10	17	13
	100	12	12	19	14
Gentamycin	-	26	28	30	28

negative) was tested using the Muller-Hinton agar and nutrient broth for the comparison with the synthesized pristine complexes, ligands, and LDHs. Details of the measurement for the antimicrobial susceptibility are described in the literature (Uddin *et al*. 2014). The perceptivity of the bacterial strains can be confirmed from the diameter of the inhibition zone (DIZ).

In general, compounds are active if clear zones around the wells exist. The DIZ can be predicted in millimeter scale.

Fig. 7 represents the formation of inhibition zones of the synthesized materials, which shows the antibacterial activity of (a) *B*. *subtilis*, (b) *E*. *coli*, (c) *S*. *aureus*, and (d) *P*. *aeroginosa* at various concentrations (25, 50, 100 μg/mL) of Ag-SMTCA-LDH. Though it is not clear to see the differences in the images, where the names of different bacterial strains and different concentrations in numbers are marked in the petri dishes, all the antibacterial activities in Fig. 7 are listed numerically in Table 2. Table 2 clearly compares the antibacterial activity of the combined metal oxides against both bacteria of *B*. *subtilis*, *S*. *aureus*, *E*. *coli*, and *P*. *aeruginosa*. Excellent antibacterial activity was observed for all the samples against both gram-positive and gram-negative bacteria. The results indicate that the complex intercalated LDH materials possess good antibacterial activity. The activities of gentamycin were reported as a positive control, whereas LDH has been used as a negative control against the bacteria. Around 10 mm and 12 mm DIZ were observed for the Ag-SMTCA-LDH and nanoparticles, respectively, by agar dilution method. We encountered that the decrease of nanoparticles size in the mixed metal oxide would facilitate the enhanced antibacterial activity. In most cases, a compound containing higher specific surface area can show better antibacterial activity. The composites retain antimicrobial activity of Ag-SMTCA-LDH.

The mechanism of inhibitory action of Ag on microorganisms is partially known. Since Ag have positive charge, it will attach with the negative charged microorganisms by the electrostatic attraction in the cell wall membrane (Dibrov *et al*. 2002). The Ag closely associated with cell wall of bacteria by forming 'pits' finally affects the permeability, and causes cell death (Sondi and Salopek-Sondi 2004). Zn/Al-LDH also exhibits excellent antibacterial activity, while Ag incorporated Zn/Al-LDH shows much enhanced antibacterial activity due to the synergistic effects of Ag and Zn/Al-LDH (Mishra *et al*. 2013). As expected, therefore, the Ag-SMTCA-LDH showed excellent antimicrobial activity against *S. aureus and P. aeruginosa* and inactive against the former strains. In general, *S. aureus and P*. *aeroginosa* are more deadly acute infections which actively react or interact with biofilms, leading to intractable chronic infections (Wang and Zhang 2012). It should be noteworthy that our synthesized materials showed excellent antibacterial activity to various bacterial strains, hinting the excellent applicability of our material as an antibacterial agent.

3.1.8 Antioxidant activity by DPPH assay

Thermal and oxidative degradation of materials usually occurs in the presence of heat and UV radiation such as in sunlight. Thus, various functional additives such as antioxidants are required to improve the thermo-oxidative stability and function of materials (Pan *et al*. 2008, Zhang *et al*. 2017). In particular, intercalated LDH nanohybrid system constructed using host–guest chemistry has been employed as multifunctional nanofiller to fabricate highly durable polymer composites with good antioxidant acitivty (Lonkar *et al*. 2013b). The antioxidant hybrid compounds were reported by intercalating low molecular weight antioxidant species into the interlayer spacing of LDHs. In comparison with organic antioxidants, intercalated antioxidants was found to have three merits: (1) the host–guest interaction effectively enhances the thermal stability of the antioxidant species; (2) the host–guest interaction prevents the migration of the antioxidant species from the LDH; (3) the inorganic–organic interface between the intercalated antioxidant and the matrix material limits the migration of the antioxidant from the matrix material (Lonkar *et al*. 2013a, b, Feng *et al*. 2014). For example, it was reported that some LDH including Zn/Al-LDH exhibits good antioxidant activity when an antioxidant agent such as 3-(3,5-di-tert-butyl-4-hydroxyphenyl)propionate(DBHP) or carnosine was intercalated (Lacikova *et al*. 2009, Kong *et al*. 2010, Lonkar *et al*. 2013a, b, Zhang *et al*. 2017). In addition, Schiff base metal complex was also reported to show good antioxidant activity (Harinath *et al*. 2013). Inspired by all those previous works, we checked the antioxidant effect of LDH, g-SMTCA, and Ag-SMTCA-LDH.

Fig. 8 illustrates dose-response bar charts for the DPPH scavenging activity of LDH, Ag-SMTCA and Ag-SMTCA-LDH, showing that all the materials showed potential free radical scavengers with powerful inhibition activity in a dose-dependent manner. Nonetheless, the inhibition of the DPPH radical scavenging activity of Ag-SMTCA-LDH increases rapidly with increasing concentration as compared with Ag-SMTCA. Interestingly, the Ag-SMTCA-LDH exhibited a maximum scavenging efficacy of 91.45% (within 30 min) at 500 mg mL^{-1}, which was much higher

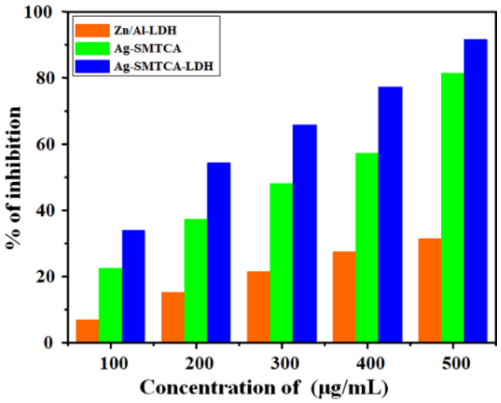

Fig. 8 The DPPH radical scavenging activity of Zn/Al-LDH, Ag-SMTCA, and Ag-SMTCA-LDH.

than that of Ag-SMTCA (85.25%). Such higher scavenging activity for DPPH is in part due to more oxidant being incorporated onto the surface of Ag-SMTCA-LDH with increasing Ag amounts owing to their high surface area. Therefore, the absorption reduction is minimal at lower concentration of Ag-SMTCA-LDH. It should be noteworthy that the intercalations of Ag-SMTCA in the LDH galleries acquire excellent antioxidant activity.

4. Conclusions

In summary, we demonstrated that the Schiff base ligand derived from sulfanilamide and 5-methyl-2-thiophene carboxaldehyde and the complexation with silver nitrate ions were successfully synthesized and confirmed the intercalation of the complex into the interlayer cavities of Zn/Al-LDH. The detailed characterization of Zn/Al-LDH confirmed the successful development of highly layered plate-like LDH nanoparticles. Further, the homogeneous Schiff base ligand was synthesized, and the complexation was carried out at mild reaction conditions. The structural analysis confirmed the successful intercalation of Ag-SMTCA-LDH antioxidant into clay galleries. The incorporation of Ag-SMTCA-LDH into LDH layers also maintained the overall morphology. The Schiff base complex intercalated into the layered structure of LDH (Ag-SMTCA-LDH) exhibited excellent activities against both gram-negative *E. coli and P. aeroginosa*, and gram-positive *S. aureus and B. subtils* bacteria's. In addition, we successfully incorporated an active antioxidant compounds into LDH galleries, which demonstrated that our method is a feasible approach in order to increase the physicochemical stability and longevity. It is assumed that the fine tuning of this active agent by intercalation and de-intercalation with different LDHs, basicity, and charge densities can make the use of the material for wider applications.

Acknowledgments

The work was supported by the National Research Foundation of Korea (NRF) Grant funded by the Ministry of Science and ICT, Korea {NRF-2017R1A2B3012961) and Brain Korea 21 Plus Program (4199990414196)).

References

Abderrazek, K., Najoua, F.S. and Srasra, E. (2016), "Synthesis and characterization of [Zn–Al] LDH: Study of the effect of calcination on the photocatalytic activity", *Appl. Clay Sci.*, **119**, 229-235. https://doi.org/10.1016/j.clay.2015.10.014

Ahmadi, R.A. and Amani, S. (2012), "Synthesis, spectroscopy, thermal analysis, magnetic properties and biological activity studies of Cu(II) and Co(II) complexes with Schiff base dye ligands", *Molecules*, **17**, 6434-6448. https://doi.org/10.3390/molecules17066434

Barbosa, C.A.S., Ferreira A.M.D.C. and Constantino, V.R.L. (2002), "Preparation and characterization of Cu (II) phthalocyanine tetrasulfonate intercalated and supported on layered double hydroxides", *J. Incl. Phenom. Macrocycl. Chem.*, **42**, 15-23. https://doi.org/10.1023/A:1014598231722

Barnabas, M.J., Parambadath, S. and Ha, C.S. (2017), "Amino modified core-shell mesoporous silica based layered double hydroxide (MS-LDH) for drug delivery", *J. Ind. Eng. Chem.*, **53**, 392-403. https://doi.org/10.1016/j.jiec.2017.05.011

Buey, J., Coco, S., Dıez, L., Espinet, P., Alvarez, J.M.M. and Miguel, J.A. (1998), "Synthesis and second-order nonlinear optical properties of new palladium(II) and platinum(II) schiff base complexes", *Organometallics*, **17**, 1750-1755. https://doi.org/10.1021/om9708900

Caboni, P., Sarais, G., Aissani, N., Tocco, G., Sasanelli, N., Liori, B., Carta, A. and Angioni, A. (2012), "Nematicidal activity of 2 thiophenecarboxaldehyde and methylisothiocyanate from caper (Capparis spinosa) against meloidogyne incognita", *J. Agric. Food Chem.*, **60**, 7345-7351. https://doi.org/10.1021/jf302075w

Cohen, S.M., Fukushima, S., Gooderham, N.J., Guengerich, F.P., Hecht, S.S., Rietjens, I.M., Smith, R.L., Bastaki, M., Harman, C.L., McGowen, M.M. and Valerio, L.G. (2017), "Safety evaluation of substituted thiophenes used as flavoring ingredients", *Food Chem. Toxicol.*, **99**, 40-50. https://doi.org/10.1016/j.fct.2016.10.023

Delahaye, É., Eyele-Mezui, S., Diop, M., Leuvrey, C., Rabu, P. and Rogez, G. (2010), "Rational synthesis of chiral layered magnets by functionalization of metal simple hydroxides with chiral and non-chiral Ni(II) Schiff base complexes", *Dalton Trans.*, **39**, 10577-10580. https://doi.org/10.1039/C0DT00834F

Dibrov, P., Dzioba, J., Gosink, K.K. and Hase, C.C. (2002), "Chemiosmoticmechanism of antimicrobial activity of Ag in Vibrio cholera", *Antimicrob. Agents Chemother.*, **46**, 2668-2670. https://doi.org/10.1128/AAC.46.8.2668-2670.2002

Ding, X., Yuan, P., Gao, N., Zhu, H., Yang, Y.Y. and Xu, Q.H. (2017), "Au-Ag core-shell nanoparticles for simultaneous bacterial imaging and synergistic antibacterial activity", *Nanomed.-Nanotechnol.*, **13**, 297-305. https://doi.org/10.1016/j.nano.2016.09.003

Feng, Y., Jiang, Y., Huang, Q., Chen, S., Zhang, F., Tang, P. and Li, D. (2014), "High antioxidative performance of layered double hydroxides/polypropyelene composite with intercalation of low-molecular weight phenolic antioxidant", *Ind. Eng. Chem. Res.*, **53**, 2287-2292. https://doi.org/10.1021/ie403643v

Ganesh, M., Aziz, A.S., Ubaidaulla, U., Hemalatha, P., Saravanakumar, A., Ravikumar, R., Peng, M.M., Choi, E.Y. and Jang, H.T. (2016), "Sulfanilamide and silver nanoparticles-loaded polyvinyl alcohol-chitosan composite electrospun nanofibers: Synthesis and evaluation on synergism in wound healing", *J. Ind. Eng. Chem.*, **39**, 127-135. https://doi.org/10.1016/j.jiec.2016.05.021

Goss, C.H.A., Henderson, W., Wilkins, A.L. and Evans, C. (2003), "Synthesis, characterization and biological activity of gold(III)

catecholate and related complexes", *J. Organomet. Chem*., **679**, 194-201. https://doi.org/10.1016/S0022-328X(03)00585-0

Harinath, Y., Reddy, D.H.K., Kumar, B.N., Apparao, Ch. and Seshaiah, K. (2013), "Synthesis, spectral characterization and antioxidant activity studies of a bidentate Schiff base, 5-methyl thiophene-2-carboxaldehyde-carbohydrazone and its Cd(II), Cu(II), Ni(II) and Zn(II) complexes", *Spectrochim. Acta. Part A Mol. Biomol. Spectros*., **101**, 264-272. https://doi.org/10.1016/j.saa.2012.09.085

Ingale, V.D., Shinde, V.G., Dighore, N.R., Rajbhoj, A.S. and Gaikwad, S.T. (2015), "Synthesis, characterization and antimicrobial activity of a bivalent schiff base derived from salicylaldehyde and 4-methoxyaniline and its lanthanides (III) complexes", *J. Chem. Pharm. Res*., **7**, 493-499.

Isa, I.M., Sohaimi, N.M., Hashim, N., Kamari, A., Mohamed, A., Ahmad, M. and Ghani, S.A. (2013), "Determination of salicylate ion by potentiometric membrane electrode based on zinc aluminium layered double hydroxides-4(2,4-dichlorophenoxy) butyrate nanocomposites", *Int. J. Electrochem. Sci*., **8**, 2112-2121.

Jamuna, K., Naik, B.R., Sreenu, B. and Seshaiah, K. (2012), "Synthesis, characterization and antibacterial activity of Cu(II) and Fe(III) complexes of a new tridentate Schiff base ligand", *J. Chem. Pharm. Res*., **4**(9), 4275-4282.

Ji, T., Chen, L., Schmitz, M., Bao, F.S. and Zhu, J. (2015), "Hierarchical macrotube/mesopore carbon decorated with mono-dispersed Ag nanoparticles as a highly active catalyst", *Green Chem*., **17**, 2515-2523. https://doi.org/10.1039/C5GC00123D

Keshk, S.M., Ramadan, A.M., Al-Sehemi, A.G. and Bondock, S. (2016), "Peculiar behavior of starch 2,3-dialdehyde towards sulfanilamide and sulfathiazole", *Carbohyd. Polym*., **152**, 624-631. https://doi.org/10.1016/j.carbpol.2016.07.061

Khanye, S.D., Wan, B., Franzblau, S.G., Gut, J., Rosenthal, P.J., Smith, G.S. and Chibale, K. (2011), "Synthesis and in vitro antimalarial and antitubercular activity of gold(III) complexes containing thiosemicarbazone ligands", *J. Organomet. Chem*., **696**, 3392-3396. https://doi.org/10.1016/j.jorganchem.2011.07.026

Khoo, T.J., bin Break, M.K., Crouse, K.A., Tahir, M.I.M., Ali, A.M., Cowley, A.R., Watkin, D.J. and Tarafder, M.T.H. (2014), "Synthesis, characterization and biological activity of two Schiff base ligands and their nickel(II), copper(II), zinc(II) and cadmium(II) complexes derived from S-4-picolyldithiocarbazate and X-ray crystal structure of cadmium(II) complex derived from pyridine-2-carboxaldehyde", *Inorg. Chim. Acta*., **413**, 68-76. https://doi.org/10.1016/j.ica.2014.01.001

Kong, X., Jin, L., Wei, M. and Duan, X. (2010), "Antioxidant drugs intercalated into layered double hydroxide: Structure and in vitro release", *Appl. Clay Sci*., **49**, 324-329. https://doi.org/10.1016/j.clay.2010.06.017

Kursunlu, A.N., Guler, E., Dumrul, H., Kocyigit, O. and Gubbuk, I.H. (2009), "Chemical modification of silica gel with synthesized new Schiff base derivatives and sorption studies of cobalt (II) and nickel (II)", *Appl. Surf. Sci*., **255**, 8798-8803. https://doi.org/10.1016/j.apsusc.2009.06.055

Lacikova, L., Jancova, M., Muselik, J., Masterova, I., Grancai, D. and Fickova, M. (2009), "Antiproliferative, cytotoxic, antioxidant activity and polyphenols contents in leaves of four Staphylea L. species", *Molecules*, **14**, 3259-3267. https://doi.org/10.3390/molecules14093259

Lonkar, S.P., Kutlu, B., Leuteritz, A. and Heinrich, G. (2013a), "Nanohybrids of phenolic antioxidant intercalated into MgAl-layered double hydroxide clay", *Appl. Clay Sci*., **71**, 8-14. https://doi.org/10.1016/j.clay.2012.10.009

Lonkar, S.P., Leuteritz, A. and Heinrich, G. (2013b), "Antioxidant intercalated layered double hydroxides: a new multifunctional nanofiller for polymers", *RSC Adv*., **3**, 1495-1501. https://doi.org/10.1039/C2RA21956E

Marcato, P.D., Parizotto, N.V., Martinez, D.S.T., Paula, A.J., Ferreira, I.R., Melo, P.S., Durán, N. and Alves, O.L. (2013), "New hybrid material nased on layered double hydroxides and biogenic silver nanoparticles: antimicrobial activity and cytotoxic effect", *J. Braz. Chem. Soc*., **24**, 266-272. http://dx.doi.org/10.5935/0103-5053.20130034

Mishra, G., Dash, B., Pandey, S. and Mohanty, P.P. (2013), "Antibacterial actions of silver nanoparticles incorporated Zn-Al layered double hydroxide and its spinel", *J. Environ. Chem. Eng*., **1**, 1124-1130. https://doi.org/10.1016/j.jece.2013.08.031

Nocchetti, M., Donnadio, A., Ambrogi, V., Andreani, P., Bastianini, M., Pietrella, D. and Latterini, L. (2013), "Ag/AgCl nanoparticle decorated layered double hydroxides: synthesis, characterization and antimicrobial properties", *J. Mater. Chem. B*, **1**, 2383-2393. https://doi.org/10.1039/C3TB00561E

Noh, W., Sun, X., Ramachandran, A., Rearick, C. and Dey, S.K. (2012), "Synthesis and characterization of silver (core)/layered double hydroxide (shell) nanoparticles", *Int. J. Mater. Sci*., **2**(3), 83-87.

Nunes, J.H.B., de Paiva, R.E.F., Cuin, A., Lustri, W.R. and Corbi, P.P. (2015), "Silver complexes with sulfathiazole and sulfamethoxazole: Synthesis, spectroscopic characterization, crystal structure and antibacterial assays", *Polyhedron*, **85**, 437-444. https://doi.org/10.1016/j.poly.2014.09.010

Özbek, N., Alyar, S., Memmi, B.K., Gündüzalp, A.B., Bahçeci, Z. and Alyar, H. (2017), "Synthesis, characterization, computational studies, antimicrobial activities and carbonic anhydrase inhibitor effects of 2-hydroxy acetophenone-N-methyl p-toluenesulfonylhydrazone and its Co(II), Pd(II), Pt(II) complexes", *J. Mol. Struct*., **1127**, 437-448. https://doi.org/10.1016/j.molstruc.2016.07.122

Pan, Y., Wang, K., Huang, S., Wang, H., Mu, X., He, C., Ji, X., Zhang, J. and Huang, F. (2008), "Antioxidant activity of microwave-assisted extract of longan (*Dimocarpus Longan* Lour.) peel", *Food Chem*., **106**, 1264-1270. https://doi.org/10.1016/j.foodchem.2007.07.033

Parida, K.M., Sahoo, M. and Singha, S. (2016), "A novel approach towards solvent-free epoxidation of cyclohexene by Ti(IV)–Schiff base complex-intercalated LDH using H_2O_2 as oxidant", *J. Catal*., **276**, 161-169. https://doi.org/10.1016/j.jcat.2010.09.012

Peng, F., Wang, D., Zhang, D., Yan, B., Cao, H., Qiao, Y. and Liu, X. (2018), "PEO/Mg-Zn-Al LDH composite coating on Mg alloy as a Zn/Mg ion-release platform with multifunctions: enhanced corrosion resistance, osteogenic, and antibacterial activities", *ACS Biomater. Sci. Eng*., **4**(12), 4112-4121. https://doi.org/10.1021/acsbiomaterials.8b01184

Prabhu, S. and Poulose, E.K. (2012), "Silver nanoparticles: mechanism of antimicrobial action, synthesis, medical applications, and toxicity effects", *Int. Nano Lett*., **2**(1), article no. 32. https://doi.org/10.1186/2228-5326-2-32

Ran, X., Wang, L., Cao, D. Lin, Y. and Hao, J. (2011), "Synthesis, characterization and in vitro biological activity of cobalt(II), copper(II) and zinc(II) Schiff base complexes derived from salicylaldehyde and D,L-selenomethionine", *Appl. Organomet. Chem*., **25**(1), 9-15. https://doi.org/10.1002/aoc.1680

Rani, M. and Mohamad, Y. (2014), "Synthesis, studies and in vitro antibacterial activity of some 5-(thiophene-2-yl)-phenyl pyrazoline derivatives", *J. Saudi Chem. Soc*., **18**, 411-417. https://doi.org/10.1016/j.jscs.2011.09.002

Ray, S., Mohan, R., Singh, J.K., Samantaray, M.K., Shaikh, M.M., Panda, D. and Ghosh, P. (2007), "Anticancer and antimicrobial metallopharmaceutical agents based on palladium, gold, and silver n-heterocyclic carbene complexes", *J. Am. Chem. Soc*., **129**, 15042-15053. https://doi.org/10.1021/ja075889z

Rasouli, N., Movahedi, M. and Doudi, M. (2017), "Synthesis and

characterization of inorganic mixed metal oxide nanoparticles derived from Zn-Al layered double hydroxide and their antibacterial activity", *Surf. Interf.*, **6**, 110-115. https://doi.org/10.1016/j.surfin.2016.11.007

Rubino, S., Busà, R., Attanzio, A., Alduina, R., Di Stefano, V., Girasolo, M.A., Orecchio, S. and Tesoriere, L. (2017), "Synthesis, properties, antitumor and antibacterial activity of new Pt(II) and Pd(II) complexes with 2,20 - dithiobis(benzothiazole) ligand", *Bioorgan. Med. Chem.*, **25**, 2378-2386. https://doi.org/10.1016/j.bmc.2017.02.067

Salehi, M., Ghasemi, F., Kubicki, M., Asadi, A., Behzad, M., Ghasemi, M.H. and Gholizadeh, A. (2016), "Synthesis, characterization, structural study and antibacterial activity of the Schiff bases derived from sulfanilamides and related copper(II) complexes", *Inorg. Chim. Acta.*, **453**, 238-246. https://doi.org/10.1016/j.ica.2016.07.028

Savić, N.D., Milivojevic, D.R., Glišić, B.Đ., Ilic-Tomic, T., Veselinovic, J., Pavic, A., Vasiljevic, B., Nikodinovic-Runic, J. and Djuran, M.I. (2016), "A comparative antimicrobial and toxicological study of gold(III) and silver(I) complexes with aromatic nitrogen-containing heterocycles: synergistic activity and improved selectivity index of Au(III)/Ag(I) complexes mixture", *RSC Adv.*, **6**, 13193-13206. https://doi.org/10.1039/C5RA26002G

Sharaby, C.M. (2007), "Synthesis, spectroscopic, thermal and antimicrobial studies of some novel metal complexes of Schiff base derived from [N1-(4-methoxy-1,2,5-thiadiazol-3-yl)sulfanilamide] and 2-thiophene carboxaldehyde", *Spectrochim. Acta. Part A Mol. Biomol. Spectros.*, **66**, 1271-1278. https://doi.org/10.1016/j.saa.2006.05.030

Shebl, M., Khalil, S.M.E., Ahmed, S.A. and Medien, H.A.A. (2010), "Synthesis, spectroscopic characterization and antimicrobial activity of mono-, bi- and tri-nuclear metal complexes of a new Schiff base ligand", *J. Mol. Struct.*, **980**, 39-50. https://doi.org/10.1016/j.molstruc.2010.06.034

Shi, H., Yu, C. and He, J. (2010), "On the structure of layered double hydroxides intercalated with titanium tartrate complex for catalytic asymmetric sulfoxidation", *J. Phys. Chem. C*, **114**, 17819-17828. https://doi.org/10.1021/jp106931g

Sondi, I. and Salopek-Sondi, B. (2004), "Silver nanoparticles as antimicrobial agent: a case study on *E. coli* as a model for Gram-negative bacteria", *J. Colloid Interf. Sci.*, **275**, 177-182. https://doi.org/10.1016/j.jcis.2004.02.012

Tenreiro, S., Alberdi, G., Martínez, J., López-Torres, M., Ortigueira, J.M., Pereira, M.T. and Vila, J.M. (2003), "New palladium(II) cyclometallated compounds derived from transcinnamalylideneimines via C-H activation of an sp2 - aliphatic carbon atom", *Inorg. Chim. Acta*, **342**, 145-150. https://doi.org/10.1016/S0020-1693(02)01156-8

Uddin, M.N., Chowdhury, D.A., Rony, M.M. and Halim, M.E. (2014), "Metal complexes of Schiff bases derived from 2-thiophenecarboxaldehyde and mono/diamine as the antibacterial agents", *Modern Chem.*, **2**(2), 6-14. https://doi.org/10.11648/j.mc.20140202.11

Ukrainczyk, L., Chibwe, M., Pinnavaia, T.J. and Boyd, S.A. (1994), "ESR study of cobalt(II) tetratis(N-methyl-4-pyridmiumyl)porphyrin and cobalt(II) tetrasulfophthalocyanine intercalated in layered aluminosilicates and a layered double hydroxide", *J. Phys. Chem.*, **98**(10), 2668-2676. https://doi.org/10.1021/j100061a026

Vanja, M. and Gurusamy, A. (2013), "Coleus aromaticus leaf extract mediated synthesis of silver nanoparticles and its bacterial activity", *Appl. Nanosci.*, **3**, 217-223. https://doi.org/10.1007/s13204-012-0121-9

Wang, Y. and Zhang, D. (2012), "Synthesis, characterization, and controlled release antibacterial behavior of antibiotic intercalated Mg-Al layered double hydroxides", *Mater. Res. Bull.*, **47**, 3185-3194. https://doi.org/10.1016/j.materresbull.2012.08.029

Wang, M.Z., Li, Y., Ji, J.J., Huang, G.L., Zhang, X., Li, S.H. and Yang, X.J. (2013), "Novel hybrids of Cu2+ ternary complexes of salicylidene-amino acid Schiff base with phenanthroline (or bipyridine) intercalated in Mg/Al-NO_3-layered double hydroxide", *Chinese Chem. Lett.*, **24**, 593-596. https://doi.org/10.1016/j.cclet.2013.03.040

Wang, H., Yuan, H., Li, S., Li, Z. and Jiang, M. (2016), "Synthesis, antimicrobial activity of Schiff base compounds of cinnamaldehyde and amino acids", *Bioorg. Med. Chem. Lett.*, **26**, 809-813. https://doi.org/10.1016/j.bmcl.2015.12.089

Yuan, X., Jing, Q., Chen, J. and Li, L. (2017), "Photocatalytic Cr(VI) reduction by mixed metal oxide derived from ZnAl layered double hydroxide", *Appl. Clay Sci.*, **143**, 168-174. https://doi.org/10.1016/j.clay.2017.03.034

Zanvettor, N.T., Abbehausen, C., Lustri, W.R., Cuin, A., Masciocchi, N. and Corbi, P.P. (2015), "Silver sulfadoxinate: Synthesis, structural and spectroscopic characterizations, and preliminary antibacterial assays in vitro", *J. Mol. Struct.*, **1082**, 180-187. https://doi.org/10.1016/j.molstruc.2014.11.004

Zanvettor, N.T., Nakahata, D.H., Paiva, R.E.F., Ribeiro, M.A., Cuin, A., Corbi, P.P. and Formiga, A.L.B. (2016), "Copper(II), palladium(II) and platinum(II) complexes with 2,2-thiophen-yl-imidazole: Synthesis, spectroscopic characterization, X-ray crystallographic studies and interactions with calf-thymus DNA", *Inorg. Chim. Acta.*, **443**, 304-315. https://doi.org/10.1016/j.ica.2016.01.011

Zhang, X., Wei, M., Pu, M., Li, X., Chen, H., Evans, D.G. and Duan, X. (2005), "Preparation and characterization of trans-RhCl(CO) $(TPPTS)_2$-intercalated layered double hydroxides", *J. Solid. State. Chem.*, **178**, 2701-2708. https://doi.org/10.1016/j.jssc.2005.06.008

Zhang, L., Xiong, Z., Li, L., Burt, R. and Zhao, X.S. (2016), "Uptake and degradation of orange II by zinc aluminum layered double oxides", *J. Colloid Interf. Sci.*, **469**, 224-230. https://doi.org/10.1016/j.jcis.2016.02.005

Zhang, Q., Jiao, Q., Leroux, F., Tang, P., Li, D. and Feng, Y. (2017), "Antioxidant intercalated Zn-containing layered double hydroxides: preparation, performance and migration properties", *New J. Chem.*, **41**, 2364-2371. https://doi.org/10.1039/C6NJ03544B

Zhao, X., Wang, L., Xu, X., Lei, X., Xu, S. and Zhang, F. (2012), "Frabrication and photocatalytic properties of novel ZnO/$ZnAl_2O_4$ nanocomposite with $ZnAl_2O_4$ dispersed inside ZnO network", *AICHE J.*, **58**, 573-582. https://doi.org/10.1002/aic.12597

JL